

Exact Pairwise Error Probability Analysis of Space-Time Codes in Realistic Propagation Environments

Tharaka A. Lamahewa[†], Marvin K. Simon^{*}, Thushara D. Abhayapala[†] and Rodney A. Kennedy[†]

[†]Department of Telecommunications Engineering, Research School of Information Sciences and Engineering, The Australian National University, Canberra ACT 0200, Australia.

^{*}Jet Propulsion Laboratory, California Institute of Technology, Pasadena, CA 91109, USA.

Abstract—In this paper, we derive an analytical expression for the exact pairwise error probability (PEP) of a space-time coded system operating over a spatially correlated slow fading channel using a moment-generating function-based approach. This analytical PEP expression is more realistic than previously published exact-PEP expressions as it fully accounts for antenna spacing, antenna geometries (Uniform Linear Array, Uniform Grid Array, Uniform Circular Array, etc.) and scattering models (Uniform, Gaussian, Laplacian, Von-mises, etc). Inclusion of spatial information provides valuable insights into the physical factors determining the performance of a space-time code. We demonstrate the strength of our new analytical PEP expression by evaluating the performance of two space-time trellis codes proposed in the literature for different spatial scenarios.

I. INTRODUCTION

Space-time coding combines channel coding with multiple transmit and multiple receive antennas to achieve bandwidth and power efficient high data rate transmission over fading channels. The performance criteria for space-time codes have been derived in [1] based on the Chernoff bound applied to the pairwise error probability (PEP). In general, the Chernoff bound is quite loose for low signal-to-noise ratios. In [2], the exact-PEP of space-time codes operating over independent and identically distributed (i.i.d.) fast fading channels was derived using the method of residues. A simple method for exactly evaluating the PEP based on the moment generating function associated with a quadratic form of a complex Gaussian random variable [3] is given in [4] for both i.i.d. slow and fast fading channels. The fading correlation effects on the performance of space-time codes were investigated in [5]. There, the exact-PEP results derived in [2] were further extended to spatially correlated slow fading channels with the use of residue methods. In [5], the correlation is calculated in terms of the correlation between channel gains, but there is no direct realizable physical interpretation to the spatial correlation. Therefore, existing PEP expressions derived in the literature do not provide insights into the physical factors determining the performance of a space-time code operating

over correlated fading channels. In particular, the effect of antenna spacing, spatial geometry of the antenna arrays and the non-isotropic scattering environments on the performance of space-time codes are of interest.

In this paper, using the MGF-based approach presented in [4], we derive an analytical expression for the exact-PEP of a space-time coded system operating over a spatially correlated slow fading channel. This expression is more realistic than previously published exact-PEP expressions, as it fully accounts for antenna placement along with non-isotropic scattering environments. Using this analytical expression one can evaluate the performance of a space-time code applied to a MIMO system in any general spatial scenario (*antenna geometries*: Uniform Linear Array (ULA), Uniform Grid Array (UGA), Uniform Circular Array (UCA), etc. *scattering models*: Uniform, Gaussian, Laplacian, Von-mises, etc.) without the need for extensive simulations. We provide an analytical technique which can be used to evaluate the exact-PEP in closed form. We demonstrate the strength of our new analytical PEP expression by evaluating the performance of a 4-state QPSK space-time trellis code with two transmit antennas proposed by *Tarokh et al.* [1] and a 16-state QPSK space-time trellis code with three transmit antennas proposed by *Zuho-Chen et al.* [6] for different spatial scenarios.

Notations: Throughout the paper, the following notations will be used: $[\cdot]^T$, $[\cdot]^*$ and $[\cdot]^\dagger$ denote the transpose, complex conjugate and conjugate transpose operations, respectively. The symbols $\delta(\cdot)$ and \otimes denote the Dirac delta function and Matrix Kronecker product, respectively. The notation $E\{\cdot\}$ denotes the mathematical expectation, $Q(y) = \int_{-\infty}^y e^{-x^2/2} dx$ denotes the Gaussian Q-function, $\text{vec}(\mathbf{A})$ denotes the vectorization operator which stacks the columns of \mathbf{A} , and $\lceil \cdot \rceil$ denotes the ceiling operator. The matrix \mathbf{I}_n is the $n \times n$ identity matrix.

II. SYSTEM MODEL

Consider a MIMO system consisting of n_T transmit antennas and n_R receive antennas. Let $\mathbf{x}_n = [x_1^{(n)}, x_2^{(n)}, \dots, x_{n_T}^{(n)}]^T$ denote the space-time coded signal vector transmitted from n_T transmit antennas in the n -th symbol interval and $\mathbf{X} = [\mathbf{x}_1, \mathbf{x}_2, \dots, \mathbf{x}_L]$ denote the space-time code representing the entire transmitted signal, where L is the code length. Assuming

This work was supported by the Australian Research Council Discovery Grant DP0343804.

Thushara D. Abhayapala and Rodney A. Kennedy are also with National ICT Australia, Locked Bag 8001, Canberra, ACT 2601, Australia. National ICT Australia is funded through the Australian Government's *Backing Australia's Ability* initiative, in part through the Australian Research Council.

quasi-static fading, the signals received at n_R receiver antennas during L symbol periods can be expressed in matrix form as

$$\mathbf{Y} = \sqrt{E_s} \mathbf{H} \mathbf{X} + \mathbf{N},$$

where E_s is the transmitted power per symbol at each transmit antenna and \mathbf{H} is the $n_R \times n_T$ zero-mean complex valued channel gain matrix, \mathbf{N} is the noise represented by an $n_R \times L$ complex matrix in which entries are zero-mean independent Gaussian distributed random variables with variance $N_0/2$ per dimension.

A. Spatial Channel Model

Using a recently developed 2-dimensional spatial channel model¹ [8], we are able to incorporate the antenna spacing, antenna placement and scattering distribution parameters such as mean angle-of-arrival (AOA), mean angle-of-departure (AOD) and angular spread, into the exact-PEP calculations of space-time coded systems. In this model, the MIMO channel \mathbf{H} is decomposed into deterministic and random parts as

$$\mathbf{H} = \mathbf{J}_R \mathbf{H}_S \mathbf{J}_T^\dagger, \quad (1)$$

where \mathbf{J}_T is the $n_T \times (2m_T + 1)$ transmit antenna array configuration matrix and \mathbf{J}_R is the $n_R \times (2m_R + 1)$ receive antenna array configuration matrix, where $(2m_T + 1)$ and $(2m_R + 1)$ are the number of effective communication modes² available in the transmitter and receiver regions, respectively. Note that, m_T and m_R are determined by the size of the antenna aperture, but not from the number of antennas encompassed in an antenna array. The number of effective communication modes (M) available at a region is given by [9]

$$M \triangleq 2 \lceil \pi e r / \lambda \rceil + 1, \quad (2)$$

where r is the minimum radius of the antenna array aperture, λ is the wavelength and $e \approx 2.7183$. We refer the reader to [8] for the definitions of \mathbf{J}_R and \mathbf{J}_T . Finally, \mathbf{H}_S is the $(2m_R + 1) \times (2m_T + 1)$ random scattering matrix with (ℓ, m) -th element given by

$$\{\mathbf{H}_S\}_{\ell, m} = \int_0^\pi \int_0^\pi g(\phi, \varphi) e^{-i(\ell - m_R - 1)\varphi} e^{i(m - m_T - 1)\phi} d\varphi d\phi, \\ \ell = 1, \dots, 2m_R + 1, \quad m = 1, \dots, 2m_T + 1 \quad (3)$$

Note that $\{\mathbf{H}_S\}_{\ell, m}$ represents the complex gain of the scattering channel between the m -th mode of the transmitter region and the ℓ -th mode of the receiver region, where $g(\phi, \varphi)$ is the scattering gain function, which is the effective random complex gain for signals leaving the transmitter aperture with angle of departure ϕ and arriving at the receiver aperture with angle of arrival φ .

¹The 2-D case is a special case of the 3-D case where all the signals arrive from on a horizontal plane only. Similar results can be obtained using the 3-D channel model proposed in [7].

²The set of modes form a basis of functions for representing a multipath wave field.

III. EXACT PEP ON CORRELATED MIMO CHANNELS

Assume that perfect channel state information (CSI) is available at the receiver and also a maximum likelihood (ML) decoder is employed at the receiver. Assume that the codeword \mathbf{X} was transmitted, but the ML-decoder chooses another codeword $\hat{\mathbf{X}}$. Then the PEP, conditioned on the channel, is given by [1]

$$P(\mathbf{X} \rightarrow \hat{\mathbf{X}} | \mathbf{h}) = Q \left(\sqrt{\frac{E_s}{2N_0}} d^2(\mathbf{X}, \hat{\mathbf{X}}) \right), \quad (4)$$

where $d^2(\mathbf{X}, \hat{\mathbf{X}}) = \mathbf{h} [\mathbf{I}_{n_R} \otimes \mathbf{X}_\Delta] \mathbf{h}^\dagger$, $\mathbf{X}_\Delta = (\mathbf{X} - \hat{\mathbf{X}})(\mathbf{X} - \hat{\mathbf{X}})^\dagger$, $\mathbf{h} = (\text{vec}(\mathbf{H}^T))^T$ is a row vector. To compute the average PEP, we average (4) over the joint probability distribution of \mathbf{h} . By using Craig's formula for the Gaussian Q-function [10, Chap. 4, Eq. (4.2)]

$$Q(x) = \frac{1}{\pi} \int_0^{\pi/2} \exp\left(-\frac{x^2}{2 \sin^2 \theta}\right) d\theta$$

and the MGF-based technique presented in [4], we can write the average PEP as

$$P(\mathbf{X} \rightarrow \hat{\mathbf{X}}) = \frac{1}{\pi} \int_0^{\pi/2} \int_0^\infty \exp\left(-\frac{\Gamma}{2 \sin^2 \theta}\right) p_\Gamma(\Gamma) d\Gamma d\theta, \\ = \frac{1}{\pi} \int_0^{\pi/2} \mathcal{M}_\Gamma\left(-\frac{1}{2 \sin^2 \theta}\right) d\theta, \quad (5)$$

where $\mathcal{M}_\Gamma(s) \triangleq \int_0^\infty e^{s\Gamma} p_\Gamma(\Gamma) d\Gamma$ is the MGF of

$$\Gamma = \frac{E_s}{2N_0} \mathbf{h} [\mathbf{I}_{n_R} \otimes \mathbf{X}_\Delta] \mathbf{h}^\dagger \quad (6)$$

and $p_\Gamma(\Gamma)$ is the probability density function (pdf) of Γ . Substituting (1) for \mathbf{H} in $\mathbf{h} = (\text{vec}(\mathbf{H}^T))^T$ and using the Kronecker product identity [11, page 180] $\text{vec}(\mathbf{A}\mathbf{X}\mathbf{B}) = (\mathbf{B}^T \otimes \mathbf{A}) \text{vec}(\mathbf{X})$, we rewrite (6) as

$$\Gamma = \frac{E_s}{2N_0} \mathbf{h}_S (\mathbf{J}_R^T \otimes \mathbf{J}_T^\dagger) (\mathbf{I}_{n_R} \otimes \mathbf{X}_\Delta) (\mathbf{J}_R^* \otimes \mathbf{J}_T) \mathbf{h}_S^\dagger, \quad (7a)$$

$$= \frac{E_s}{2N_0} \mathbf{h}_S \left[(\mathbf{J}_R^\dagger \mathbf{J}_R)^T \otimes (\mathbf{J}_T^\dagger \mathbf{X}_\Delta \mathbf{J}_T) \right] \mathbf{h}_S^\dagger, \quad (7b)$$

$$= \frac{E_s}{2N_0} \mathbf{h}_S \mathbf{G} \mathbf{h}_S^\dagger, \quad (7c)$$

where $\mathbf{h}_S = (\text{vec}(\mathbf{H}_S^T))^T$ is a row vector and

$$\mathbf{G} = (\mathbf{J}_R^\dagger \mathbf{J}_R)^T \otimes (\mathbf{J}_T^\dagger \mathbf{X}_\Delta \mathbf{J}_T). \quad (8)$$

Note that, (7b) follows from (7a) via the identity [11, page 180] $(\mathbf{A} \otimes \mathbf{C})(\mathbf{B} \otimes \mathbf{D}) = \mathbf{AB} \otimes \mathbf{CD}$, provided that the matrix products \mathbf{AB} and \mathbf{CD} exist.

Note that $\mathbf{h}_S \mathbf{G} \mathbf{h}_S^\dagger$ in (7c) is a quadratic form of a random variable since \mathbf{h}_S is a random row vector and \mathbf{G} is fixed as $\mathbf{J}_T, \mathbf{J}_R$ and \mathbf{X}_Δ are deterministic matrices. Furthermore, the matrix \mathbf{G} is Hermitian as both $\mathbf{J}_R^\dagger \mathbf{J}_R$ and $\mathbf{J}_T^\dagger \mathbf{X}_\Delta \mathbf{J}_T$ are Hermitian, and the Kronecker product between two Hermitian matrices is always Hermitian. The MGF associated with a quadratic random variable is readily found in the literature [3]. Using [3, Eq. 14], we write the MGF of Γ as

$$\mathcal{M}_\Gamma(s) = \left[\det \left(\mathbf{I} - \frac{s\bar{\gamma}}{2} \mathbf{R}\mathbf{G} \right) \right]^{-1}, \quad (9)$$

where $\bar{\gamma} = \frac{E_s}{N_0}$ is the average symbol energy-to-noise ratio and $\mathbf{R} = E \{ \mathbf{h}_S^\dagger \mathbf{h}_S \}$ is the covariance matrix of \mathbf{h}_S . Here we assumed that the entries of \mathbf{h}_S are zero-mean complex Gaussian distributed.

Substitution of (9) into (5) gives the exact-PEP

$$P(\mathbf{X} \rightarrow \hat{\mathbf{X}}) = \frac{1}{\pi} \int_0^{\pi/2} \left[\det \left(\mathbf{I} + \frac{\bar{\gamma}}{4 \sin^2 \theta} \mathbf{R} \mathbf{G} \right) \right]^{-1} d\theta. \quad (10)$$

Remark 1: Eq. (10) is the exact-PEP³ of a space-time coded system applied to a spatially correlated slow fading MIMO channel following the channel decomposition in (1).

Remark 2: When $\mathbf{R} = \mathbf{I}$ (i.e., correlation between different communication modes is zero), Eq. (10) above captures the effects due to antenna spacing and antenna geometry on the performance of a space-time code operating over a slow fading channel.

Remark 3: When the fading channels are independent (i.e., $\mathbf{R} = \mathbf{I}$ and $\mathbf{G} = \mathbf{I}_{n_R} \otimes \mathbf{X}_\Delta$), (10) simplifies to,

$$P(\mathbf{X} \rightarrow \hat{\mathbf{X}}) = \frac{1}{\pi} \int_0^{\pi/2} \prod_{n=1}^L \left[\det \left(\mathbf{I}_{n_T} + \frac{\bar{\gamma}}{4 \sin^2 \theta} \mathbf{X}_\Delta \right) \right]^{-n_R} d\theta,$$

which is the same as [4, Eq. (13)].

A. Kronecker Product Model as a Special Case

In some circumstances, the covariance matrix \mathbf{R} of the scattering channel \mathbf{H}_S can be expressed as a Kronecker product between correlation matrices observed at the receiver and the transmitter antenna arrays [12, 13], i.e.,

$$\mathbf{R} = E \{ \mathbf{h}_S^\dagger \mathbf{h}_S \} = \mathbf{F}_R \otimes \mathbf{F}_T, \quad (11)$$

where \mathbf{F}_R and \mathbf{F}_T are the transmit and receive correlation matrices. Substituting (11) in (10) and recalling the definition of \mathbf{G} in (8), the exact-PEP can be written as

$$P(\mathbf{X} \rightarrow \hat{\mathbf{X}}) = \frac{1}{\pi} \int_0^{\pi/2} \left[\det \left(\mathbf{I} + \frac{\bar{\gamma}}{4 \sin^2 \theta} \mathbf{Z} \right) \right]^{-1} d\theta \quad (12)$$

where $\mathbf{Z} = (\mathbf{F}_R \mathbf{J}_R^T \mathbf{J}_R^*) \otimes (\mathbf{F}_T \mathbf{J}_T^\dagger \mathbf{X}_\Delta \mathbf{J}_T)$.

IV. REALISTIC EXACT-PEP

The exact-PEP expression we derived in the previous section captures the antenna configurations (Linear Array, Circular Array, Grid, etc.) both at the transmitter and the receiver arrays via \mathbf{J}_T and \mathbf{J}_R , respectively. Furthermore, it also incorporates the spatial correlation effects at the transmitter and the receiver regions via \mathbf{F}_T and \mathbf{F}_R , respectively. Therefore, the PEP expression (12) can be considered as the *realistic* exact PEP of a space-time coded system.

To calculate the exact-PEP, one needs to evaluate the integral (12) (or (10) in a more general spatial scenario), either using numerical methods or analytical methods. We present an analytical technique which can be employed to evaluate the integral (12) in closed form as follows.

³Eq. (10) can be evaluated in closed form using the analytical technique discussed in Section IV.

Matrix \mathbf{Z} in (12) has size $M_R M_T \times M_R M_T$, where $M_R = 2m_R + 1$ and $M_T = 2m_T + 1$. Therefore, the integrand in (12) will take the form⁴

$$\left[\det \left(\mathbf{I} + \frac{\bar{\gamma}}{4 \sin^2 \theta} \mathbf{Z} \right) \right]^{-1} = \frac{(\sin^2 \theta)^N}{\sum_{\ell=0}^N a_\ell (\sin^2 \theta)^\ell}, \quad (13)$$

where $N = M_R M_T$ and a_ℓ , for $\ell = 1, 2, \dots, N$, are constants. Note that the denominator of (13) is an N -th order polynomial in $\sin^2 \theta$. To evaluate the integral (13) in closed form, we use the partial-fraction expansion technique given in [10, Appendix 5A] as follows.

First we begin by factoring the denominator of (13) into terms of the form $(\sin^2 \theta + c_\ell)$, for $\ell = 1, 2, \dots, N$. This involves finding the roots of an N -th order polynomial in $\sin^2 \theta$ either numerically or analytically. Then (13) can be expressed in product form as

$$\frac{(\sin^2 \theta)^N}{\sum_{\ell=0}^N a_\ell (\sin^2 \theta)^\ell} = \prod_{\ell=1}^{\Lambda} \left(\frac{\sin^2 \theta}{c_\ell + \sin^2 \theta} \right)^{m_\ell} \quad (14)$$

where m_ℓ is the multiplicity of the root c_ℓ and $\sum_{\ell=1}^{\Lambda} m_\ell = N$. Applying the partial-fraction decomposition theorem to the product form (14), we get

$$\prod_{\ell=1}^{\Lambda} \left(\frac{\sin^2 \theta}{c_\ell + \sin^2 \theta} \right)^{m_\ell} = \sum_{\ell=1}^{\Lambda} \sum_{k=1}^{m_\ell} A_{k\ell} \left(\frac{\sin^2 \theta}{c_\ell + \sin^2 \theta} \right)^k \quad (15)$$

where the residual $A_{k\ell}$ is given by [10, Eq. 5A.72]

$$A_{k\ell} = \frac{\left\{ \frac{d^{m_\ell-k}}{dx^{m_\ell-k}} \prod_{\substack{n=1 \\ n \neq \ell}}^{\Lambda} \left(\frac{1}{1 + c_n x} \right)^{m_n} \right\} \Big|_{x=-c_\ell^{-1}}}{(m_\ell - k)! c_\ell^{m_\ell - k}}. \quad (16)$$

Expansion (15) often allows integration to be performed on each term separately by inspection. In fact, each term in (15) can be separately integrated using a result found in [4], where

$$\begin{aligned} P(c_\ell, k) &= \frac{1}{\pi} \int_0^{\pi/2} \left(\frac{\sin^2 \theta}{c_\ell + \sin^2 \theta} \right)^k d\theta, \\ &= \left[1 - \sqrt{\frac{c_\ell}{1 + c_\ell}} \sum_{j=0}^{k-1} \binom{2j}{j} \left(\frac{1}{4(1 + c_\ell)} \right)^j \right]. \end{aligned} \quad (17)$$

Now using the partial-fraction form of the integrand in (15) together with (17), we obtain the exact-PEP in closed form as

$$\begin{aligned} P(\mathbf{X} \rightarrow \hat{\mathbf{X}}) &= \frac{1}{\pi} \int_0^{\pi/2} \prod_{k=1}^{\Lambda} \left(\frac{\sin^2 \theta}{c_\ell + \sin^2 \theta} \right)^{m_\ell} d\theta, \\ &= \frac{1}{2} \sum_{\ell=1}^{\Lambda} \sum_{k=1}^{m_\ell} A_{k\ell} P(c_\ell, k). \end{aligned} \quad (18)$$

⁴One would need to evaluate the determinant of $\left(\mathbf{I} + \frac{\bar{\gamma}}{4 \sin^2 \theta} \mathbf{Z} \right)$ and then take the reciprocal of it to obtain the form (13).

For the special case of distinct roots, i.e., $m_1 = m_2 = \dots = m_N = 1$, the exact-PEP is given by

$$P(\mathbf{X} \rightarrow \hat{\mathbf{X}}) = \frac{1}{2} \sum_{\ell=1}^N \left(1 - \sqrt{\frac{c_\ell}{1+c_\ell}} \right) \prod_{\substack{n=1 \\ n \neq \ell}}^N \left(\frac{c_\ell}{c_\ell - c_n} \right).$$

V. ANALYTICAL PERFORMANCE EVALUATION: EXAMPLES

In this section, we consider the following two space-time codes as examples.

- 4-state QPSK space-time trellis code with two transmit antennas [1, Fig. 4]; the shortest error event path of length $H = 2$, as illustrated by shading in Fig. 1 of [4].
- 16-state QPSK space-time trellis code with three transmit antennas [6, Table 1]; the shortest error event path of length $H = 3$.

For the 4-state code, the exact-PEP results and approximate BEP results for $n_R = 1$ and $n_R = 2$ were presented in [2, 4] for i.i.d. fast fading and slow fading channels. In [5], the effects of fading correlation on the average BEP were studied for $n_R = 1$ over a slow fading channel. In this work, we compare the i.i.d. channel performance results presented in [2, 4] with our realistic exact-PEP results for different antenna spacing and scattering distribution parameters. In addition, we use the 16-state code with three transmit antennas to study the impact of antenna placement on the performance of space-time codes.

In [2, 4], performances were evaluated under the assumption that the transmitted codeword is the all-zero codeword. Here we also adopt the same assumption as we compare our results with their results. However, we are aware that space-time codes may, in general, be non-linear, i.e., the average BEP can depend on the transmitted codeword.

A. Effect of Antenna Spacing

First we consider the effect of antenna spacing on the exact-PEP when the scattering environment is uncorrelated, i.e., $\mathbf{F}_T = \mathbf{I}_{2M_T+1}$ and $\mathbf{F}_R = \mathbf{I}_{2M_R+1}$. Consider the 4-state code with two transmit antennas and two receive antennas, where the two transmit antennas are placed in a circular aperture of radius 0.25λ (antenna separation⁵ = 0.5λ) and the two receive antennas are placed in a circular aperture of radius r (antenna separation = $2r$).

Fig.1 shows the exact pairwise error probability performance of the 4-state code for $H = 2$ and receive antenna separations 0.1λ , 0.2λ , 0.5λ and λ . Also shown in Fig.1 for comparison is the exact-PEP for the i.i.d. slow fading channel (Rayleigh) corresponding to the length two error event path.

As we can see from the figure, the effect of antenna separation on the exact-PEP is not significant when the receive antenna separation is 0.5λ or higher. However, the effect is

⁵In a 3-D isotropic scattering environment, antenna separation 0.5λ (first null of the order zero spherical Bessel function) gives zero spatial correlation, but here we constraint our analysis to a 2-D scattering environment. The spatial correlation function in a 2-D isotropic scattering environment is given by a Bessel function of the first kind. Therefore, antenna separation $\lambda/2$ does not give zero spatial correlation in a 2-D isotropic scattering environment.

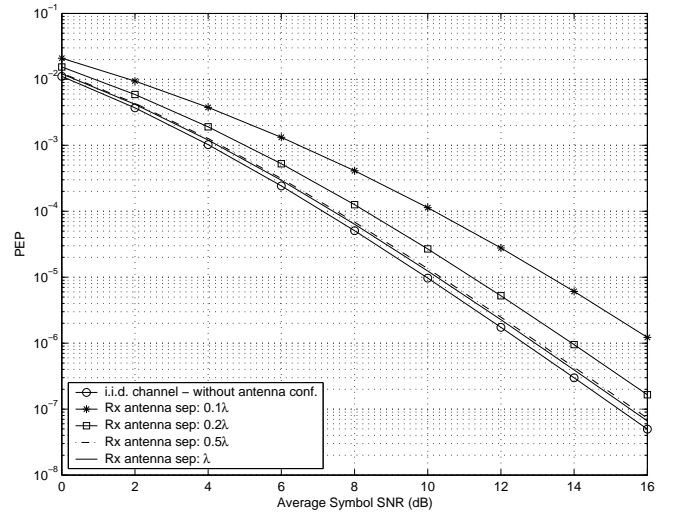


Fig. 1. Exact pairwise error probability performance of the 4-state space-time trellis code with 2-Tx antennas and 2-Rx antennas: length 2 error event.

significant when the receive antenna separation is small. For example, at 0.2λ and 0.1λ receive antenna separations, the realistic PEPs are 1dB and 3dB away from the i.i.d. channel performance results, respectively. From these observations, we can emphasize that the effect of antenna spacing on the performance of the 4-state code is minimum for higher antenna separations whereas the effect is significant for smaller antenna separations.

B. Effect of Antenna Configuration

In this section, we compare the PEP performance of the 16-state code for different antenna configurations at the transmitter antenna array. Here we consider UCA and ULA antenna configurations as examples.⁶ We place the three transmit antennas within a fixed circular aperture of radius r ($= 0.15\lambda, 0.25\lambda$), where the antenna placements are shown in Fig.2. The exact-PEP performance for the error event path of length three is also shown in Fig 2 for a single receive antenna.

From Fig.2, it is observed that at high SNRs the performance given by the UCA antenna configuration outperforms that of the ULA antenna configuration. For example, at 14dB SNR, the performance differences between UCA and ULA are 1.75dB with 0.15λ transmitter aperture radius and 1dB with 0.25λ transmitter aperture radius.

According to the performance criteria given in [1], the slope of the performance curve on a log scale corresponds to the diversity advantage of the code and the horizontal shift in the performance curve corresponds to the coding advantage. From Fig.2, we observed that as the radius of the transmitter aperture decreases the diversity advantage of the code is reduced, particularly for the ULA antenna configuration. Here, the loss of diversity advantage is mainly due to the loss of rank of \mathbf{J}_T , as is shown in [14].

⁶The exact-PEP expression we derived in this work can be applied to any arbitrary antenna configuration.

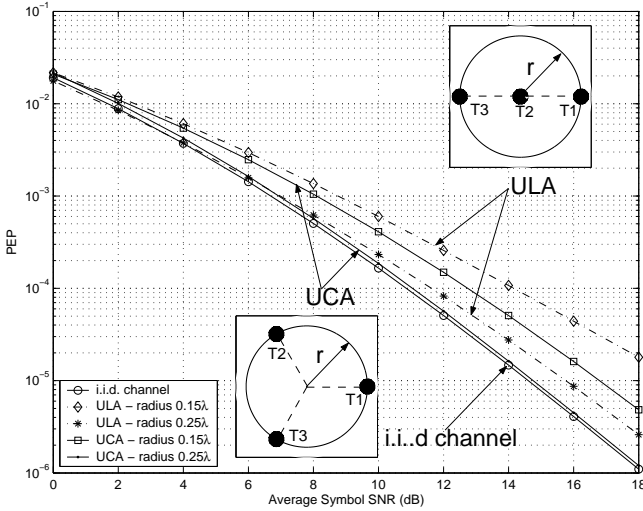


Fig. 2. The exact-PEP performance of the 16-state code with three transmit and one receive antennas for UCA and ULA transmit antenna configurations: length 3 error event.

C. Effect of Modal Correlation

For simplicity, here we only consider the modal correlation effects at the receiver region and assume that the effective communication modes available at the transmitter region are uncorrelated, i.e., $\mathbf{F}_T = \mathbf{I}_{2M_T+1}$. First, we derive the definition of modal correlation matrix \mathbf{F}_R at the receiver region.

Using (3), we can define the modal correlation between complex scattering gains as

$$\gamma_{m,m'}^{\ell,\ell'} \triangleq E \left\{ \{ \mathbf{H}_S \}_{\ell,m} \{ \mathbf{H}_S \}_{\ell',m'}^* \right\}.$$

Assume that the scattering from one direction is independent of that from another direction for both the receiver and the transmitter apertures. Then the second-order statistics of the scattering gain function $g(\phi, \varphi)$ can be defined as

$$E \left\{ g(\phi, \varphi) g^*(\phi', \varphi') \right\} = G(\phi, \varphi) \delta(\phi - \phi') \delta(\varphi - \varphi'),$$

where $G(\phi, \varphi) = E \left\{ |g(\phi, \varphi)|^2 \right\}$ with normalization $\int \int G(\phi, \varphi) d\phi d\varphi = 1$. With the above assumption, the modal correlation coefficient, $\gamma_{m,m'}^{\ell,\ell'}$ can be simplified to

$$\gamma_{m,m'}^{\ell,\ell'} = \int \int G(\phi, \varphi) e^{-i(\ell-\ell')\varphi} e^{i(m-m')\phi} d\phi d\varphi.$$

Then the correlation between the ℓ -th and ℓ' -th modes at the receiver region due to the m -th mode at the transmitter region is given by

$$\gamma_{\ell,\ell'}^{Rx} = \int \mathcal{P}_{Rx}(\varphi) e^{-i(\ell-\ell')\varphi} d\varphi, \quad (19)$$

where $\mathcal{P}_{Rx}(\varphi) = \int G(\phi, \varphi) d\phi$ is the normalized azimuth power distribution of the scatterers surrounding the receiver antenna region. Here we see that modal correlation at the receiver is independent of the mode selected from the transmitter region. Note that the (ℓ, ℓ') -th element of \mathbf{F}_R is given by (19) and \mathbf{F}_R is a $(2m_R + 1) \times (2m_R + 1)$ matrix. Also note that $\mathcal{P}_{Rx}(\varphi)$ can be modeled using all common azimuth

power distributions such as Uniform, Gaussian, Laplacian, Von-Mises, Polynomial, etc.

It was shown in [15] that all azimuth power distribution models give very similar correlation values for a given angular spread, especially for small antenna separations. Therefore, without loss of generality, we restrict our investigation only to the case of energy arriving uniformly over a limited angular spread σ around a mean AOA φ_0 (uniform limited azimuth power distribution). In this case, the modal correlation coefficient $\gamma_{\ell,\ell'}^{Rx}$ in the receiver region is given by

$$\gamma_{\ell,\ell'}^{Rx} = \text{sinc}((\ell - \ell')\sigma) e^{-i(\ell-\ell')\varphi_0}. \quad (20)$$

Continuing the performance analysis, we now investigate the modal correlation effects on the performance of the 4-state code with two transmit and two receive antennas. We place the two transmit antennas 0.5λ apart and also the two receive antennas 0.5λ apart.⁷

Fig. 3 shows the exact-PEP performances of the 4-state code for various angular spreads $\sigma = \{5^\circ, 30^\circ, 45^\circ, 180^\circ\}$ about a mean AOA $\varphi_0 = 0^\circ$ from broadside, where the broadside angle is defined as the angle perpendicular to the line connecting the two antennas. Note that $\sigma = 180^\circ$ represents the isotropic scattering environment. The exact-PEP performance for the i.i.d. slow fading channel (Rayleigh) is also plotted on the same graph for comparison.

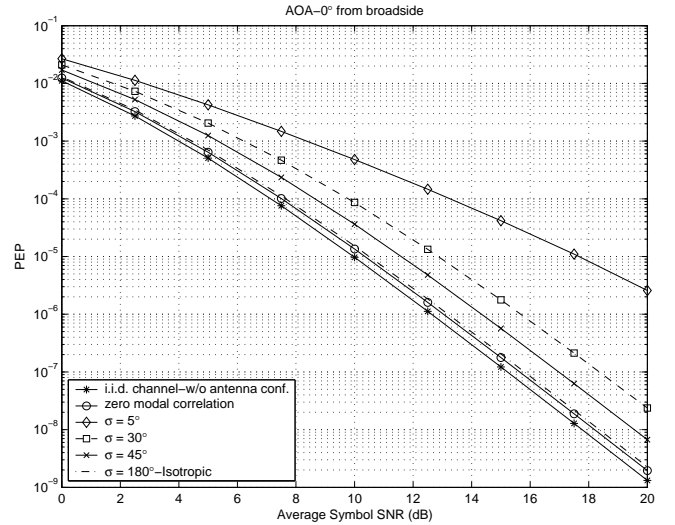


Fig. 3. Effect of receiver modal correlation on the exact-PEP of the 4-state QPSK space-time trellis code with 2-Tx antennas and 2-Rx antennas for the length 2 error event. Uniform limited power distribution with a mean angle of arrival $\varphi_0 = 0^\circ$ from broadside and angular spreads $\sigma = \{5^\circ, 30^\circ, 45^\circ, 180^\circ\}$.

As one would expect, the performance loss incurred due to the modal correlation increases as the angular spread of the distribution decreases. For example, at 10dB SNR, the realistic PEP performance results obtained from (12) are 0.25dB, 1.5dB, 2.75dB and 7.5dB away from the i.i.d. channel performance results for angular spreads $180^\circ, 45^\circ, 30^\circ$ and 5° , respectively. Therefore, in general, if the angular spread of

⁷Performance loss due to antenna spacing is minimum when the antenna separation is 0.5λ or higher as we showed in Section V-A

the distribution is closer to 180° (isotropic scattering), then the loss incurred due to the modal correlation is insignificant, provided that the antenna spacing is optimal. However, for moderate angular spread values such as 45° and 30° , the performance loss is quite significant. This is due to the higher concentration of energy closer to the mean AOA for small angular spreads. It is also observed that for large angular spread values, the diversity order of the code (the slope of the performance curve) is preserved whereas for small and moderate angular spread values, the diversity order of the code is diminished.

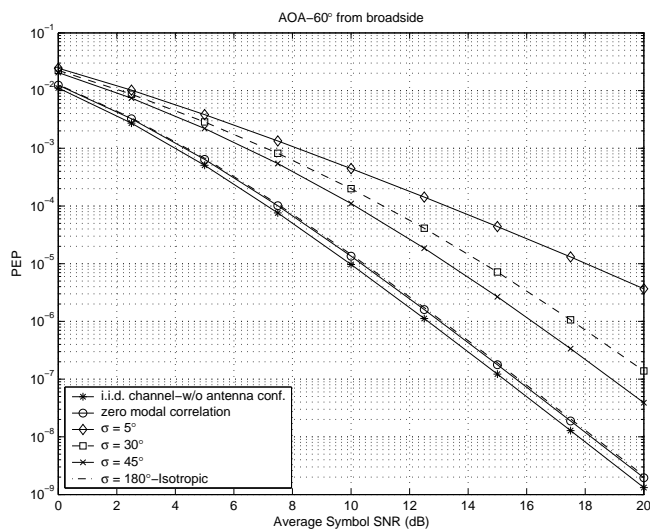


Fig. 4. Effect of receiver modal correlation on the exact-PEP of the 4-state QPSK space-time trellis code with 2-Tx antennas and 2-Rx antennas for the length 2 error event. Uniform limited power distribution with a mean angle of arrival $\varphi_0 = 60^\circ$ from broadside and angular spreads $\sigma = \{5^\circ, 30^\circ, 45^\circ, 180^\circ\}$.

Fig.4 shows the PEP performance results of the 4-state code for a mean AOA $\varphi_0 = 60^\circ$ from broadside. Similar results are observed as for the mean AOA $\varphi_0 = 0^\circ$ case. Comparing Figs. 3 and 4 we observe that the performance loss is increased for all angular spreads as the mean AOA moves away from broadside. This can be justified by the reasoning that, as the mean AOA moves away from broadside, there will be a reduction in the angular spread exposed to the antennas and hence less signals being captured.

Furthermore, we observed that (performance results are not shown here) when there are more than two receive antennas in a fixed receiver aperture, the performance loss of the 4-state code with decreasing angular spread is most pronounced for the ULA antenna configuration when the mean AOA is closer to 90° (inline with the array). But, for the UCA antenna configuration, the performance loss is insignificant as the mean AOA moves away from broadside for all angular spreads. This suggests that the UCA antenna configuration is less sensitive to change of mean AOA compared to the ULA antenna configuration. Hence, the UCA antenna configuration is best suited to employ a space-time code.

Using the results we obtained thus far, we can claim that, in general, space-time trellis codes are susceptible to spatial fading correlation effects, in particular, when the antenna

separation and the angular spread are small.

VI. CONCLUSION

Using an MGF-based approach, we have derived an analytical expression for the exact pairwise error probability of a space-time coded system over a spatially correlated slow fading channel. This analytical PEP expression fully accounts for antenna separation, antenna geometry and surrounding azimuth power distributions, both at the receiver and the transmitter antenna arrays. In practice, it can be used as a tool to estimate or predict the performance of a space-time code under any antenna configuration and surrounding azimuth power distribution parameters. Based on this new PEP expression, we showed that space-time codes employed on multiple transmit and multiple receive antennas are susceptible to spatial fading correlation effects, particularly for small antenna separations and small angular spreads.

REFERENCES

- [1] V. Tarokh, N. Seshadri, and A.R. Calderbank, "Space-time codes for high data rate wireless communication: performance criterion and code construction," *IEEE Trans. Info. Theory*, vol. 44, no. 1, pp. 744–765, Mar. 1998.
- [2] M. Uysal and C. N. Georghiades, "Error performance analysis of spacetime codes over rayleigh fading channels," *J. Commun. Networks*, vol. 2, no. 4, pp. 351–355, Dec. 2000.
- [3] G.L. Turin, "The characteristic function of hermetian quadratic forms in complex normal random variables," *Biometrika*, vol. 47, no. 1/2, pp. 199–201, June 1960.
- [4] M.K. Simon, "Evaluation of average bit error probability for space-time coding based on a simpler exact evaluation of pairwise error probability," *International Journal on Communications and Networks*, vol. 3, no. 3, pp. 257–264, Sept. 2001.
- [5] M. Uysal and C. N. Georghiades, "Effect of spatial fading correlation on performance of space-time codes," *Electronics Letters*, vol. 37, no. 3, pp. 181–183, Feb. 2001.
- [6] Z. Chen, B. Vucetic, J. Yuan, and K.L. Lo, "Space-time trellis codes with two, three and four transmit antennas in quasi-static flat fading channels," in *Proc. IEEE Int. Conf. Communications*, New York, NY, May 2002, pp. 1589–1595.
- [7] T.D. Abhayapala, T.S. Pollock, and R.A. Kennedy, "Novel 3d spatial wireless channel model," in *IEEE Semiannual Vehicular Technology Conference, VTC2003-Fall*, Oct 2003.
- [8] T.D. Abhayapala, T.S. Pollock, and R.A. Kennedy, "Spatial decomposition of MIMO wireless channels," Paris, France, July 2003, vol. 1, pp. 309–312.
- [9] H.M. Jones, R.A. Kennedy, and T.D. Abhayapala, "On dimensionality of multipath fields: Spatial extent and richness," in *Proc. IEEE Int. Conf. Acoust., Speech, Signal Processing, ICASSP'2002*, Orlando, Florida, May 2002, vol. 3, pp. 2837–2840.
- [10] M.K. Simon and M.-S. Alouini, *Digital Communications over Fading Channels*, John Wiley & Sons, second edition, to be available November 2004.
- [11] Gene H. Golub and Charles F. Van Loan, *Matrix Computations*, The Johns Hopkins University Press, Baltimore and London, third edition, 1996.
- [12] J.P. Kermaol, L. Schumacher, K.I. Pedersen, P.E. Mogensen, and F. Frederiksen, "A stochastic mimo radio channel model with experimental validation," *IEEE Journal on Selected Areas in Communications*, vol. 20, no. 6, pp. 1211–1226, Aug. 2002.
- [13] T.S. Pollock, "Correlation Modelling in MIMO Systems: When can we Kronecker?," in *Proc. 5th Australian Communications Theory Workshop*, Newcastle, Australia, February 2004, pp. 149–153.
- [14] T.A. Lamahewa, T.D. Abhayapala, and R.A. Kennedy, "Effect of transmit antenna configuration on rank-determinant criteria of space-time trellis codes," in *IEEE International Symposium on Spread Spectrum Techniques and Applications, ISSSTA 2004 (to appear)*, Sydney, Australia, September 2004.
- [15] T.S. Pollock, T.D. Abhayapala, and R.A. Kennedy, "Introducing space into MIMO capacity calculations," *Journal on Telecommunications Systems*, vol. 24, no. 2, pp. 415–436, 2003.